*Original Research*

# Study on Impact of Climate Change and Sea Water Intrusion on Water Quality Parameters of Coastal Area – GIS Based Research

**Senthil Kumar M.[1]\*, Muralikrishnan R.[2], Sivarethinamohan R.[3], Abdulkareem M. Matar[4]**

[1]Department of Biotechnology, Karpaga Vinayaga College of Engineering and Technology, Chengalpattu, Tamil Nadu – 603 308, India
[2]Jei Mathaajee College of Engineering, Kanchipuram to Arakkonam road, Kooram Gate, Vishakandikuppam, Kanchipuram District, Tamil Nadu – 631 552, India
[3]Symbiosis Centre for Management Studies, Symbiosis International (Deemed University), Bangaluru, India
[4]Department of Animal Production, College of Food and Agriculture Sciences, King Saud University, P.O. Box 2460, Riyadh 11451, Saudi Arabia

## Abstract

This study aims to evaluate Rameshwaram's groundwater quality in terms of seawater intrusion. The pH ranged from 6.87 to 7.82, and The EC varied between 0.81 and 13.73, 90% below the allowable limit, TDS observed at 240 mg/L to 4103 mg/L with a significance of 70% in the permitted threshold, The range of the Ca hardness was 60 mg/L to 355 mg/L, with 58% exceeding the limit, the range of the Mg hardness was 50 mg/L to 560 mg/L, with 93% surpassing the permitted limit, and the range of the TH ranged from 180 mg/L to 915 mg/L, with 30% exceeding the limit. F- concentrations range from 1 mg/L to 1.78 mg/L, showing 35% are at harmful fluoride levels, while TS concentrations range from 330 mg/L to 4100 mg/L, with over 65% above the limit. According to statistical explanations by rotating component matrix, component 1 achieved 48.53%, component 2 reached 67.64%, and component 3 reached 90.52%. Under Kaiser normalization, the minimum Varimax value fell within the range of 0.81-330.0. The range of possible Varimax values is 8.73 to 25000.60. The standard deviation varied from 0.3264 to 3867.6154, while the mean deviation ranged from 1.8373 to 1661.0150. An identity of 65% found in one group remaining 35% in another cluster. GIS-based spatiotemporal values of water quality metrics confirm the intervention of sea water intrusion in coastal zone. In conclusion, investigation of water quality in the coastal region exhibits the seawater intrusion problem with supporting results of statistical analysis and GIS mapping.

**Keywords:** coastal ground water, water quality, sea water intrusion, Rameshwaram, GIS

\*e-mail: senthilenvtce@gmail.com

## Introduction

Groundwater has traditionally been used as a source of drinking water, and it remains vital today. Ground water development has offered significant socioeconomic benefits to civilization [1]. It is projected to provide around 50% of existing drinking water supplies globally. Most people assume that groundwater is reasonably pure and free of pollution. Although most groundwater is still of high quality, there are notable exceptions, The purity of groundwater is becoming increasingly difficult to preserve [2]. Seawater intrusions are a major source of groundwater pollution. Saltwater intrusion in groundwater aquifers can be exacerbated by rising sea levels combined with increased groundwater pumping [3]. Ingress of saltwater into groundwater aquifers can raise treatment costs for drinking water facilities or leave groundwater wells inoperable. The coastal shore of Rameshwaram has focused attention on groundwater removal from aquifers during the previous decade. This is due to increased water demands from a growing population, as well as a climate change problem, particularly along coastal shallow groundwater in Rameshwaram coastline zone and Salinization of groundwater in drilled wells and deep boreholes is a serious challenge in drinking water quality and residential water supply management in the coastal region of Rameshwaram [4]. The primary goal of this research is to undertake a comprehensive assessment of the quality of groundwater resources in the Rameshwaram coastal zone. To classify groundwater in the area of spatial water quality classes, a strong water quality index (WQI) weighted for the main factors in domestic water quality evaluation. The samples were collected and tested to determine the water quality and the extent of seawater intrusion. The rotating component matrix is used to provide statistical interpretations [5], The primary analysis of principal component analysis is utilized to assess the correlation between each variable created by the water quality analysis, and kaiser normalization illustrations are used to anticipate the correlations between parameters and components, which are followed by box plots, which draw the lower and upper water quality parameters as horizontal lines either side of a rectangle shape, and dendrogram analyses, which provide the output in hierarchical cluster form overlay mapping using a Geographical Information System (GIS) in a comprehensive approach to visually identify the dispersion of water quality parameters revealed polluted areas for sustainable coastal resource management [6].

Groundwater has historically been a key source of drinking water and continues to be so today. Seawater intrusion poses a serious threat to the coastal ecosystem, especially considering the increased demand for groundwater by residents of coastal metropolitan areas. The environmental threats that the seawater intrusion phenomenon poses have been investigated by several scientists from around the world. Seawater incursions are a significant cause of groundwater pollution in coastal areas [7]. Rising sea levels and greater groundwater pumping may make saltwater intrusion in groundwater aquifers worse. Although most groundwater is still of high quality, there are notable exceptions, The purity of groundwater is becoming increasingly difficult to preserve in sea shore areas [8]. Groundwater wells may become inoperable or incur higher treatment expenses as a result of saltwater intrusion into groundwater aquifers. When groundwater levels fall below the mean sea level, the hydraulic gradient is reversed and seawater in the coastal aquifer is pushed to flow inland. The growth of industry and agriculture in the region is hampered by seawater intrusion, but it also lowers people's quality of life.

Climate change and sea level rise are the two most important climatic factors that control seawater intrusion in coastal areas. Sea levels rise as a result of an increase in ocean temperature brought on by global warming, which also speeds up glacier melting. A rise in sea level results in the migration of the freshwater-seawater mixing zone to inland regions, which also raises the seawater head at the ocean's edge. Human activity is another crucial factor; it has the greatest direct and indirect impact on all other factors that regulate seawater intrusion [9]. Overuse of groundwater resources is the most significant human-caused factor speeding up seawater intrusion in coastal zones. When groundwater with a significantly higher salt content is used in agricultural fields in areas where freshwater is under severe stress, the soil eventually becomes salinized [10]. Because it is challenging and not advantageous to remove salts from the soil, the saline soil becomes unusable for agricultural activities. Groundwater usage for agriculture, land reclamation, haphazard shrimp aquaculture, inland saltpans, inadequate or poorly maintained infrastructure, and inefficient water management systems, may cause the coastal aquifer to become salinized.

The coastal shore of Rameshwaram focused attention on groundwater removal from aquifers during the previous decade. This is due to increased water demands from a growing population, as well as a climate change problem, particularly along coastal shallow groundwater in Rameshwaram coastline zone and Salinization of groundwater in drilled wells and deep boreholes is a serious challenge in drinking water quality and residential water supply management in the coastal region of Rameshwaram [11]. The primary goal of this research is to undertake a comprehensive assessment of the quality of groundwater resources in the Rameshwaram coastal zone. The rotating component matrix and kaiser normalization illustrations are used to anticipate the correlations between parameters and components, which are followed by box plots and dendrogram analyses provide the output in hierarchical cluster form used to provide statistical interpretations, Overlay mapping using a Geographical Information System (GIS) in a comprehensive approach to visually

identify the dispersion of water quality parameters revealed polluted areas for sustainable coastal resource management.

## Materials and Methods

### Study Area

Rameshwaram is a popular pilgrimage site in India. People come from all over the world to seek salvation and moksha. This research region is in the Indian state of Tamil Nadu, in the southeast [12]. At the point of the Indian peninsula, this location is separated from Sri Lanka by a narrow Palk Bay canal known as the Gulf of Mannar. The area is located between longitudes 79°12'30"E and 79°21'30"E, and latitudes 9°8'55"N to 9°19'25"N, with Pamban Bridge to the north and the Gulf of Mannar to the south [13]. Fig. 1 depicted an actual visual map of the research area. Rameshwaram is governed by a municipality that was created in 1994. The town has a total size of 53 km$^2$ (20 sq mi). The majority of Rameshwaram workforce is employed in tourism and fishing [14]. The expansion of such activities necessitates a coordinated strategy for the use and development of water resources. Rameshwaram's weather is hot, humid, windy, and cloudy. Throughout the year, the temperature normally ranges from 77ºF to 89ºF, with temperatures rarely falling below 75ºF or rising over 92ºF. The island is in a semi-arid zone where intermittent rains may occur [15]. A severe drought or a lack of rainfall can last for several years in some cases. This region is subject to two monsoons: the southwest monsoon from June to August and the northeast monsoon from October to December [16]. During the monsoon season, this area receives an average of 94 cm of rain. Cyclones are widespread in the coastal region, and they can have disastrous consequences. In recent years, pollution has become a major source of coral damage. This is due to rising population settlements in coastal towns in the Palk Bay region, which dump their untreated domestic and industrial pollutants into the oceans [17]. Tidal effect dominates pollutant load dilution around the island.

### Sample Collection and Analysis

Ground water samples were collected from 40 selected bore wells during the southwest and northeast monsoons within a 20km radius of the coastline at appropriate distance intervals designated by the Tamil Nadu Water Supply and Drainage (TWARD) board for drinking and household uses [18]. Water samples were collected in pre-sanitized plastic containers. The physical properties were measured using calibrated digital equipment at the sampling site. The chemical constituents were evaluated in a laboratory utilizing American Public Health Association (APHA) and Bureau of Indian Standards (BIS) standard procedures [19]. At the time of sampling, the physicochemical parameters of water were assessed in the field using portable meters (electrical conductivity, pH, and temperature). GPS was utilized to record the latitude and longitude of the sample collecting site.

### Water Quality Analysis

Standard techniques were used to examine water quality characteristics [20]. Temperature was recorded during sample collection using a thermometer, and
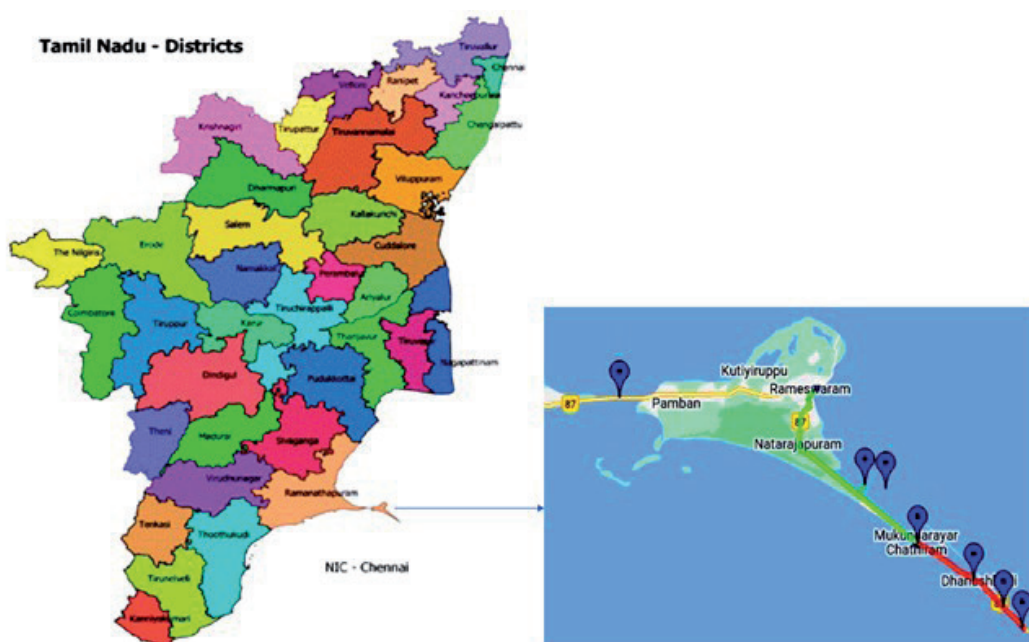


Fig. 1. Location map of study area.

Table 1. Various water quality parameters and approximated standards methods.

| S. No | Parameters | Unit | Test method |
|---|---|---|---|
| 1 | Temperature | ºC | Thermometer |
| 2 | pH | – | pH meter |
| 3 | EC | µS/cm | Digital conductivity meter |
| 4 | TDS | mg/L | Digital meter |
| 5 | Calcium | mg/L | EDTA Titration |
| 6 | Magnesium | mg/L | EDTA Titration |
| 7 | Total hardness | mg/L | EDTA Titration |
| 8 | Fluoride | mg/L | Selective ion electrode analysis |

specifics of several procedures important to parameters are presented in Table 1.

## Statistical Analysis

### *Principle Component Matrix*

SPSS software 14.0 was used to do statistical computations. Principal component analysis (PCA) is a useful approach for attempting to explain the variation of a large dataset of intercorrelated variables with a smaller collection of independent variables [21]. The eigenvalues and eigenvectors of the original variables are extracted using the PCA technique from the covariance matrix. The uncorrelated variables obtained by multiplying the original correlated variables with the eigenvector, which is a list of coefficients, are known as the Principal Components (PC) [22]. As a result, the PCs are linear weighted combinations of the original variables. PC gives information on the most important factors that describe the entire data collection while allowing for data reduction with minimal loss of original information [23]. The first major component is the linear combination of the original variables that provides the most variance to their overall variance. The residual variance is maximized by the second principal component, which is uncorrelated with the first, and so on until the total variance is examined [24]. Due to the method's reliance on the total variance of the original variables, it works best when all variables are measured in the same units.

### *Rotation Method by Varimax with Kaiser Normalization*

A varimax rotation condenses a sub-expression space into a few key elements. The real coordinate system remains unaltered, and the orthogonal basis is rotated to align with them [25]. Principal component analysis or factor analysis generate a dense subspace with several non-zero weights, making it challenging to comprehend. A subspace-invariant rotation is required for orthogonality. A variable has a high loading on a single factor but near-zero loadings on the remaining factors, while a factor is composed of only a few variables with extremely high loadings on this factor while the rest variables have near-zero loadings on this factor [26]. Kaiser normalization was used to identify potential sources. In PCA, an eigenvalue greater than one was used to select factors, and factor scores greater than 0.5 were considered significant. For all statistical analyses, a minimum significance level of 95% was adopted.

### *Cluster Analysis (CA)*

Cluster analysis is a multivariate statistical technique that allows objects to be assembled based on their similarity. CA classifies things so that each object in the cluster is like the rest in the cluster in terms of a given selection criterion [27]. The most prevalent CA method is Rescaled Distance cluster combine cluster analysis. which, generally depicted by a dendrogram, shows intuitive similarity relationships between each one sample and the entire dataset [28]. The dendrogram is a visual representation of the clustering processes and providing a representation of the groupings and their vicinity with a dramatic reduction in the original data's dimensionality.

### *GIS Mapping*

Geographical analysis with GIS was used to capture the geographical variation of ground water quality in the research area. Toposheets for 40 sampling places were created for the creation of data bases [29]. Based on the location data, a location map of the study area has been created, with point features representing the position of 40 sample areas identified and a map for the same. To characterize surface reflectance, atmospheric correction removes the scattering and absorption effects from the environment [30]. Radiometric correction is used to reduce or rectify mistakes in satellite data's digital values. The non-spatial database was prepared and evaluated in the laboratory using normal processes [31]. The ground WQI value

was determined for each sampling point. The acquired ground water quality data serves as the attribute database for the current study. The produced spatial and non-spatial (attribute) data bases were combined to create spatial distribution maps of all water quality metrics, including the WQI map [32]. To build various thematic maps, the water quality data (non-spatial data) is linked to the sample location (spatial data).

## Result and Discussion

### Water Quality Analysis

The pH values, which averaged 7.6 and 7.5, mirrored the slightly alkaline quality of the water samples. The pH recorded in the Palkulam Nelli site was acidic, ranging between 6.87 and 6.88. Table 2 shows the sample location of Edayarvalsai bond with the greatest pH level of 8.73. All the sample's pH levels were within the federal environmental protection agency and WHO guidelines [33]. Most of the samples were more than 7 levels alkaline, and the recurring likeness of alkalinity of sea water suggests sea water intrusions.

According to experimental results, the EC in CMRI, Mandabam site was greater than 13.73mg/L. The recorded range in Gandhi Nagar South Street-R-II was 10.12 mg/L, and the EC range in Mandapam Residence was around 10.58 mg/L. These three areas represent the EC alarm range, indicating that saltwater incursion persists. In general, the degree of water mineralisation in the direction of flow increases significantly. The highest EC values were found in three places in the east and along the seashore, whereas the lowest values were found in the west away from the sea level, indicating an increase in EC owing to seawater intrusion.

The Table 2 shows that TDS, as a main indicator of water quality, ranged between 240 and 2840 mg/L for all samples. 70% of the samples above the acceptable level set by WHO and the federal environmental protection agency. The TDS value range was 4103 mg/L at CMRI, Mandabam, which is close to the coastal area, while the lowest range was reported in Lotus Pond, which is west of the coastal zone. The wide range of TDS parameters listed in (Table 2) suggest that multiple pollution sources influence groundwater quality in the research area. Topography may be one of the credited variables that caused high TDS in coastal region groundwater sources [34]. The high TDS level in coastal groundwater is thought to be caused by a high rate of evapotranspiration and limited fresh water exchange, which leads to the creation, transport, and dissolution of salt layers in the research area.

Calcium hardness ($Ca^{2+}$) predominates in all tested wells, particularly those near the coast, according to analyses. The ion concentration ranges from 60 to 355 mg/L. The mixing of fresh groundwater with seawater along the shore and in coastal transition zones may be the principal sources of calcium in

aquifer systems [35]. The greatest range measured was 355 mg/L in CMRI, Mandabam, and the lowest range anticipated was 60 mg/L in the vicinity of Edaiyarvalsai Pond, as exposed in Table 2.

The concentration of Magnesium (Mg) ion in the zone costal region ranges from 50 to 560 mg/l, as shown in the Table 2. The greatest amount was 560 mg/L in CMRI, Mandabam, while the lowest level was around 50 mg/L in Maravatti valasai opposite. The primary source of magnesium hardness may be local rocks, The magnesium hardness in the coastal zone aquifer is implied by the erosion and transportation of rock components by waves in the seashore area. However, in some areas of the test region, the magnesium may be caused by the mixing of fresh groundwater with seawater along the shore.

The experimental study reveals a low range of 180 mg/L and a high value of 915 mg/L in the CMRI, Mandabam area, as revealed in the Table 2. On the other hand, overall hardness is connected to $Ca^{2+}$ and $Mg^{2+}$ ions, and calcium found in greater abundance than magnesium in numerous groundwater samples from the island and mainland locations. When seawater enters a fresh water aquifer, cation exchange occurs, with sodium being taken up by the exchanger and $Ca^{2+}$ being discharged into groundwater. Significant fresh water degradation occurs in the study region as a result of abandoned or inadequately constructed wells and the development of saline water tanks for fish preservation [36]. This exchange mechanism eventually leaves a trace of high hardness in groundwater. Total hardness implies that all the samples were very hard.

The total solids represent the suspended and dissolved solids in the obtained sample. The laboratory studies show the total solids range in representative samples, as shown in the Table 2. The experimental study revealed the lowest range was 375 mg/L in Maravatti valasai opposite and the highest value was 4100 mg/L in CMRI,Mandabam region, from the experimental data 80% of the samples reveal Nacl type water, indicating that the sample locations are near the coastline and that there is an increase in Nacl ions in the groundwater due to seawater movement towards the landside [37]. The fact that 17% of the samples are freshwater implies that they are from the recharge zone, whereas the rest samples are mixed saline ($Ca^{2+}$ -$Mg^{2+}$ -Cl type). A low carbonate concentration with a comparatively high Cl and Mg concentration implies a rising rate of solid content in the water sample. It occurs as a result of saline water intrusion into the groundwater aquifer caused by the seashore's effect.

The fluoride concentration in 59% of the samples above the WHO standard of 0.5-1.5 mg/L, whereas the remaining 41% were under the limit. The highest concentrations of fluoride were found in three locations: Palkulam, Kunjarvalasai-R, and Edaiyarvalasai, as shown in Table 2. The lowest levels were found in Enmanagundam, where they were in the 1.0mg/L range.

Table 2. Water quality characteristics of coastal zone of Rameshwaram.

| Sl. No | Name of the location | Latitude | Longitude | pH | EC | TDS mg/L | Ca Hardness mg/L | Mg Hardness mg/L | Total hardness mg/L | Total Solids mg/L | F-Level mg/L |
|---|---|---|---|---|---|---|---|---|---|---|---|
| 1. | Utchipulli S.M colony | 9' 26' 16.3'' | 79' 24.16' 18'' | 7.31 | 2.87 | 853.00 | 275.0 | 125.0 | 450.00 | 1000.0 | 1.60 |
| 2. | Maravatti valasai | 9.26' 24' 32'' | 79.11' 13' 12'' | 7.15 | 1.69 | 508.00 | 250.0 | 75.00 | 325.00 | 590.00 | 1.68 |
| 3. | Maravatti valasai Opposite | 9.15' 53.20'' | 79' 6' 45.17'' | 7.27 | 0.92 | 270.00 | 275.0 | 50.00 | 325.00 | 375.00 | 1.68 |
| 4. | Kuppani valasai | 9' 22' | 79' 21' | 7.17 | 2.45 | 725.00 | 160.0 | 185.0 | 345.00 | 750.00 | 1.60 |
| 5. | S.Valasai | 9' 26' 53.20'' | 79' 21' 41.13' | 7.26 | 1.30 | 382.00 | 150.0 | 180.0 | 330.00 | 450.00 | 1.50 |
| 6. | Lotus pond | 9' 27' 23.20'' | 79' 18' 31.15'' | 7.82 | 0.89 | 264.00 | 65.00 | 150.0 | 215.00 | 330.00 | 1.68 |
| 7. | Pirappinvalasai | 9' 30' 27.15'' | 79' 18' 39.23'' | 7.05 | 3.59 | 1085.0 | 265.0 | 255.0 | 520.00 | 1500.0 | 1.60 |
| 8. | Palkulam | 9' 42' 23.07'' | 80' 02' 01.13'' | 7.00 | 1.21 | 363.00 | 135.0 | 165.0 | 300.00 | 450.00 | 1.78 |
| 9. | Palkulam Nelli | 9' 42' 22.12'' | 80' 2' 8.27'' | 6.87 | 1.21 | 357.00 | 195.0 | 80.00 | 275.00 | 395.00 | 1.60 |
| 10. | Kulanachiyamman koil | 9' 50' 8.23'' | 81' 8' 2.43'' | 7.20 | 2.19 | 647.00 | 155.0 | 100.0 | 255.00 | 750.00 | 1.75 |
| 11. | Sundaramadaiyan | 10' 2' 10.42'' | 81' 32' 7.52'' | 7.03 | 1.01 | 300.00 | 115.0 | 160.0 | 275.00 | 440.00 | 1.68 |
| 12. | Sundaramadaiyan Bus stop | 9' 53' 10.37'' | 81' 5' 33.28'' | 7.22 | 2.56 | 756.00 | 150.0 | 150.0 | 300.00 | 920.00 | 1.50 |
| 13. | Nadumunaikadu | 9' 57' 11.57'' | 81' 9' 13.11'' | 7.40 | 1.60 | 475.00 | 115.0 | 210.0 | 325.00 | 600.00 | 1.56 |
| 14. | Kunjarvalasai-L | 10' 1' 12.32'' | 81' 37' 8.30'' | 7.03 | 1.52 | 450.00 | 175.0 | 195.0 | 370.00 | 620.00 | 1.68 |
| 15. | Kunjarvalasai-R | 10' 7' 11.40'' | 81' 34' 9.43'' | 7.01 | 1.28 | 381.00 | 225.0 | 110.0 | 335.00 | 460.00 | 1.78 |
| 16. | Kunjarvalasai pond | 10' 7' 2'' | 81' 33' 42.30'' | 7.26 | 0.91 | 268.00 | 90.00 | 150.0 | 240.00 | 380.00 | 1.60 |
| 17. | Edaiyarvalsai | 10' 5' 32.68'' | 81' 28' 40.13'' | 6.95 | 2.22 | 658.00 | 100.0 | 200.0 | 300.00 | 800.00 | 1.78 |
| 18. | Edaiyarvalsai Pond | 10' 7' 33.04'' | 81' 40' 52.56'' | 8.73 | 1.10 | 1194.0 | 60.00 | 330.0 | 390.00 | 1200.0 | 1.78 |
| 19. | Valayarpaadi | 10' 8' 37.28'' | 81' 53' 40.02'' | 7.21 | 4.43 | 1323.0 | 235.0 | 95.00 | 320.00 | 1400.0 | 1.30 |
| 20. | Naganathar Temple | 10' 10' 40.16'' | 81' 59' 38.18'' | 7.16 | 1.76 | 521.00 | 170.0 | 225.0 | 395.00 | 550.00 | 1.68 |
| 21. | Maraikayarpattinam | 11' 23' 15.12'' | 84' 12' 13.10'' | 7.18 | 3.36 | 924.00 | 250.0 | 300.0 | 550.00 | 1050.00 | 1.40 |
| 22. | Maraikayarpattinam near sea | 10' 14' 12.12'' | 82' 8' 12.08'' | 7.32 | 4.64 | 1393.0 | 160.0 | 290.0 | 450.00 | 1400.0 | 1.50 |
| 23. | CMRI,Mandabam | 14' 12' 13.01'' | 84' 12' 14.18'' | 7.01 | 13.73 | 4103.0 | 355.0 | 560.0 | 915.00 | 4100.0 | 1.40 |
| 24. | Kendravidyalayam school | 11' 8' 14.10'' | 82' 20' 10.07'' | 7.55 | 7.19 | 2148.0 | 225.0 | 215.0 | 440.00 | 2250.0 | 1.40 |
| 25. | Jail Street,Pamban | 8' 38' 15.71'' | 77' 41' 31.68'' | 7.06 | 5.45 | 1620.0 | 355.0 | 245.0 | 600.00 | 1800.0 | 1.50 |
| 26. | Near Pamban Bridge | 8' 40' 13.08'' | 77' 46' 30.53'' | 7.16 | 3.09 | 918.00 | 220.0 | 380.0 | 600.00 | 1000.0 | 1.50 |
| 27. | Park in Pamban | 8' 43' 8.13'' | 77' 48' 15.18'' | 7.39 | 2.73 | 805.00 | 200.0 | 160.0 | 360.00 | 950.00 | 1.30 |

Table 2. Continued.

| No. | Location | | | | | | | | | | |
|---|---|---|---|---|---|---|---|---|---|---|---|
| 28, | Fisherman colony-I | 8' 63' 20.35" | 79' 12' 18.03" | 7.68 | 2.64 | 782.00 | 160.0 | 165.0 | 325.00 | 800.00 | 1.10 |
| 29. | Fisherman colony-II | 8' 65' 18.05" | 79' 18' 13.12" | 7.64 | 0.81 | 240.00 | 85.00 | 95.00 | 180.00 | 350.00 | 1.25 |
| 30. | Fisherman colony-III | 8' 64' 17.33" | 79' 15' 12.56" | 7.50 | 2.17 | 640.00 | 220.0 | 130.0 | 350.00 | 700.00 | 1.40 |
| 31. | Gandhi Nagar south street-L-I | 8' 62' 13.08" | 79' 14' 11.14" | 7.52 | 1.94 | 584.00 | 145.0 | 155.0 | 300.00 | 600.00 | 1.40 |
| 32. | Gandhi Nagar south street-R-II | 8' 63' 14.13" | 79' 15' 36.50" | 7.24 | 10.12 | 3021.0 | 300.0 | 315.0 | 615.00 | 3100.0 | 1.60 |
| 33. | Mandapam near railway station | 9' 10' 12.14" | 79' 10' 14.12" | 7.10 | 3.95 | 1183.0 | 185.0 | 290.0 | 475.00 | 1200.0 | 1.68 |
| 34. | Mandapam Aiyyapan temple | 9' 12' 13.04" | 79' 13' 8.01" | 6.89 | 5.00 | 1494.0 | 280.0 | 295.0 | 575.00 | 1560.0 | 1.50 |
| 35. | Mandapam post office-L-I | 9' 14' 11.59" | 79' 14' 9.10" | 7.04 | 7.14 | 2140.0 | 150.0 | 305.0 | 455.00 | 2410.0 | 1.50 |
| 36. | Mandapam post office-R-II | 9' 14' 18.40" | 79' 14' 30.08" | 6.99 | 5.30 | 1577.0 | 300.0 | 275.0 | 575.00 | 1800.0 | 1.10 |
| 37. | Mandapam camp scan net | 9' 24' 19.20" | 79' 23' 12.11" | 7.13 | 4.35 | 1279.0 | 225.0 | 275.0 | 500.00 | 1400.0 | 1.10 |
| 38. | Pirappinvalasai-II | 9' 40' 20.12" | 79' 42' 11.12" | 7.40 | 1.22 | 358.00 | 150.0 | 100.0 | 250.00 | 500.00 | 1.10 |
| 39. | Enmanagundam | 10' 20' 12.46" | 83' 15' 12.18" | 6.95 | 1.39 | 414.00 | 190.0 | 145.0 | 335.00 | 510.00 | 1.00 |
| 40. | Mandapam Residence | 9' 45' 12.03" | 77' 49' 8.13" | 7.34 | 10.58 | 2840.0 | 350.0 | 360.0 | 610.00 | 2000.6 | 1.50 |

Fluoride's impact to groundwater in these samples is minor [38]. Fluoride levels in natural waters are low as a result of its tendency to be fixed by the nature of ground water and to be impacted by the increasing amount of fluoride. The fluoride level in groundwater sources appeared to indicate that most of the samples were unfit for drinking. As the sources at the coast are dominated by permanent fluoride pollution, particularly with high input from sea water intrusion.

## Statistical Analysis

### Rotation Component Matrix

Table 3 shows the major component analyses for the water quality analysis of the coastal area. It contains the loading for the rotated component matrix as well as the eigenvalues for each component, each component accounts for a certain percentage and a cumulative percentage of the variance were explained. It shows that the first three major components account for 90.52% of the total variation in the dataset. where the first major component accounts for 48.53% and the second principal component accounts for 67.64%. The third major component accounts for 90.52% of the overall variance [39]. The first three principal components' eigenvalues can be utilized to assess the primary hydro geochemical processes. Positive loadings of pH, $Ca^{2+}$, and TS are high (0.441-0.891), although Mg concentrations are low. For the first principal component, TH and F- have low positive loadings (0.846-0.889) (Joseph Dien et al., 2005). The values of EC and TDS for the third main component reveal high loadings of (–0.248- –0.221). $Ca^{2+}$ values suggest a modest loading rate (2.867-02). pH, TDS, Mg, $Ca^{2+}$, and TH concentrations demonstrate a low loading rate of (–0.248- –0.258).

### Varimax with Kaiser Normalization

Table 4 expressed the Varimax with Kaiser Normalization for a coastal zone water sample. It comprises the varimax matrix's loading, the valid N points for each component, the minimum, maximum, mean, and standard deviation per cent of varimax explained with Kaiser Normalization. It indicates that the first three varimax components account for 37 of the total variances in the dataset [40]. where the minimum Varimax data with Kaiser Normalization value ranged from 0.81-330.0. Varimax values might range from 8.73 to 25000.60. The mean deviation ranged from 1.8373 to 1661.0150, while the standard deviation ranged from 0.3264 to 3867.6154. The primary hydrogeochemical processes can be accessed via statistical analysis. The presence of high positive loading concentrations of pH, EC, TDS, $Ca^{2+}$, Mg, TH, TS, and F- suggests the possibility of a sea water intrusion problem.

Table 3. Rotated Component Matrix.

| | Component | | |
|---|---|---|---|
| | 1 | 2 | 3 |
| pH | .145 | -.849 | 8.4980-02 |
| EC | .950 | 4.6235-02 | -.248 |
| TDS | .962 | 3.8052-02 | -.221 |
| $Ca^{2+}$ | .441 | .770 | 2.8672-02 |
| Mg | .846 | .156 | .258 |
| TH | .811 | .461 | .198 |
| TS | .891 | .150 | .149 |
| F- | .889 | -6.2941-02 | -.334 |
| Eigen values | 5.24 | 3.13 | 2.98 |
| % age of variance by component | 48.53 | 27.36 | 23.45 |
| Cumulative %age of variance | 48.53 | 67.64 | 90.52 |

Table 4. Extraction Method: Principal Component Analysis, Rotation Method: Varimax with Kaiser Normalization - Descriptive Statistics.

| | N | Minimum | Maximum | Mean | Std. Deviation |
|---|---|---|---|---|---|
| pH | 40 | 6.87 | 8.73 | 7.2547 | .3264 |
| EC | 40 | .81 | 90.28 | 5.3302 | 14.0321 |
| TDS | 40 | 240.00 | 22840.00 | 1506.0750 | 3549.3393 |
| $Ca^{2+}$ | 40 | 330.00 | 25000.60 | 1661.0150 | 3867.6154 |
| Mg | 40 | 175.00 | 750.00 | 395.6250 | 136.5659 |
| TH | 40 | 60.00 | 355.00 | 196.6250 | 77.5290 |
| TS | 40 | 50.00 | 660.00 | 213.6250 | 123.1894 |
| F- | 37 | 1.00 | 14.00 | 1.8373 | 2.0660 |
| Valid N (listwise) | 37 | | | | |

*Cluster Analysis*

This research looked at, Cluster analysis revealed a substantial regional and temporal connection based on fluctuations in major pollution indicators, indicating that the effects of sea water incursion on water quality varied spatially and temporally. The dendrogram depicts the level of pollution as well as the impact of contamination at the sampling sites. It depicts the groupings and their proximity, providing a visual summary of the clustering processes [41]. To find similarities between the forty sampling sites, cluster analysis was utilized. Cluster analysis produced a dendrogram, which classified the sample based on the percentage of similarity and dissimilarity of water quality indicators. The percentage similarity dendrogram of forty research sites in Fig. 2 depicts based on physicochemical considerations. The similarity of research sites was analyzed to determine the degree of relationships between sites

as a cluster. The rescaled proximity cluster similarity analysis indicated an identity of 65% in one set of forty sampling locations and 35% in the remaining group. In contrast to these sites considering, it is located at the head of the stream, it has the greatest dissimilarity to other sites throughout the whole research period. Hence, the seawater intrusion has a significant impact on the seashore. Fig. 2 shows the dendrogram of percentage seasonal similarity. The dendrogram developed categorized the sampling sites based on water quality characteristics.

Interpretation by ArcGIS

The current study attempted to evaluate and map the groundwater quality surrounding Rameshwaram's coastline zone. The estimated WQI is a simple technique to understand the overall effect of seawater intrusion [42]. The integration of several thematic layers using ArcGIS
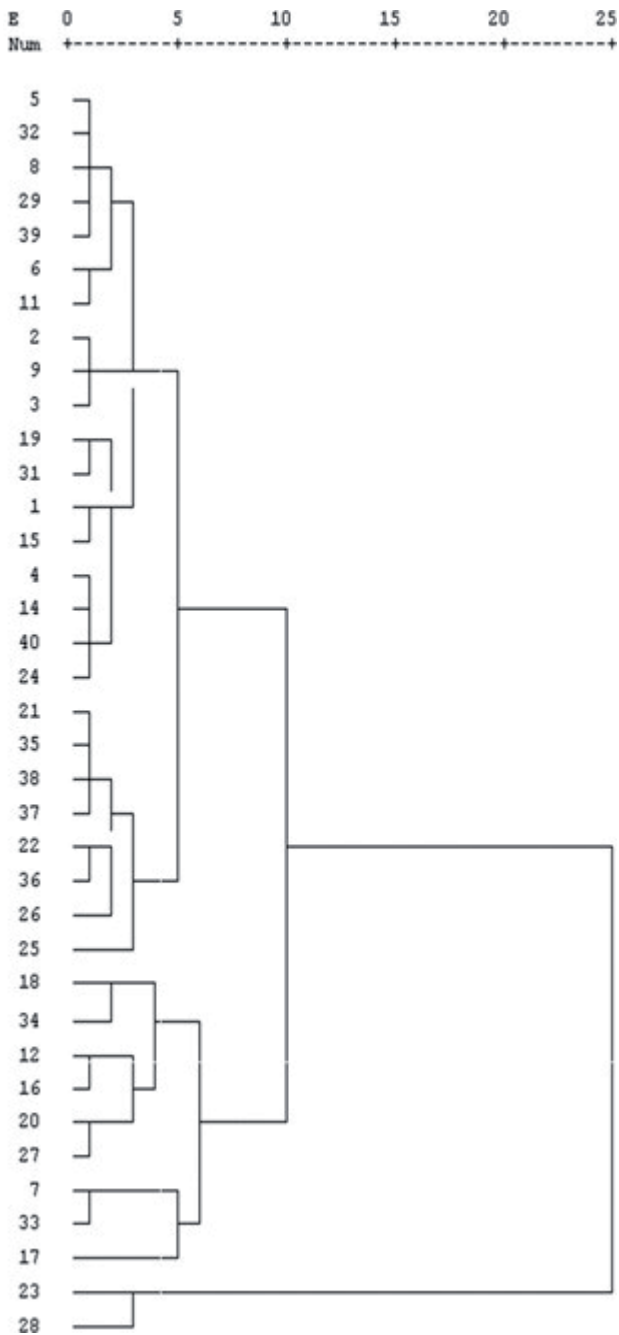
Fig. 2. Heirarchical Cluster Analysis - Dendrogram using Average Linkage (Between Groups).

9.3 is quite beneficial in establishing the acceptability of ground water quality for drinking purposes. The surface water determinant concentration in the donor region is indicated in the geographic variation maps interpolated for pH. The pH concentration is determined by the findings of the laboratory analysis, it was subsequently superimposed on the Palkulam Nelli research was acidic, ranging between 6.87 and 6.88. Fig. 3a) depicts the map interpretation of the sample site of Edayarvalsai bond with the highest pH level of 8.73 in alkaline nature distribution.

The EC specifies how salt and iron-free water may contain additional contaminants. From the results, the downstream places near the seashore had greater concentration values of 4.43 mg/L and 4.63 mg/L, whereas the western part of some areas had higher concentrations of 13.73 mg/L. The high EC concentration can be due to the limited mobility of water; as a result, EC concentration tends to rise. For EC concentration, the average lower values of EC were detected between upstream and downstream locations that operate as open water runoff. Also, Fig. 3b) shows that the receiving zone is more contaminated than the donating region in terms of EC concentration, which is well represented in the interpolated map.

Fig. 3c) depicts the geographic maps interpolated for TDS concentration in open water in the research area's coastline zone. TDS exhibits a variable pattern, and its concentration is the result of laboratory analysis findings overlaid on the research area shapefile. TDS is a broad indicator of the quality of water. Most of the study area has TDS levels ranging from 240 mg/L to 805 mg/L. The slightly higher number showed the presence of contamination caused by seawater intrusion. The interpolated map clearly shows the TDS spread.

The presence of minerals associated with rock surfaces is primarily accountable to produce calcium hardness in water. Some areas had high calcium concentrations. Fig. 3d) depicts the spatial distribution of calcium hardness ($Ca^{2+}$). Most of the location calcium hardness ranges from 60 mg/L to 195 mg/L. The greater value from the range of 355 mg/L was obtained in some sites. The precision of $Ca^{2+}$ distribution in sampling areas is shown on the GIS interpolated map.

Most of the locations were discovered to be above the permitted range of 90-400 mg/L. However, in the CMRI, Mandabam area, the highest magnesium hardness was reported in the range of 560 mg/L, while much of the area magnesium hardness (Mg) ranges from 100 mg/L to 195 mg/L. Fig. 3e) represents the spatial distribution of Mg on a GIS map, regarding Total hardness the CMRI, Mandabam area has a high concentration of total hardness in the range of 915 mg/L. Most of the region was within the ideal level, ranging from 215 mg/L to 475 mg/L. Fig. 3f) represents the spatial distribution of Total Hardness.

Higher solid content observed mostly as a result of sewage effluent overapplication, septic tanks, open solid waste dump sites, and so on [43]. A higher level of solid content, around 4100mg/L, was not discovered in the research area at CMRI, Mandabam region. Total solid content ranges from 330 mg/L to 1800 mg/L. Fig. 3g) denotes the spatial distribution of total solids.

Fluoride dissolved through geological formation is commonly found in ground water. Most of the sampling sites were within the allowable level of 1.5mg/L. Fluoride levels in some areas surpass the allowable limit, as seen in the Fig. 3h). The highest level of fluoride detected was 1.78 mg/L in Edaiyarvalsai and in Edaiyarvalsai pond [44]. Fluoride poisoning can cause disorders such as dental fluorosis and skeletal fluorosis.
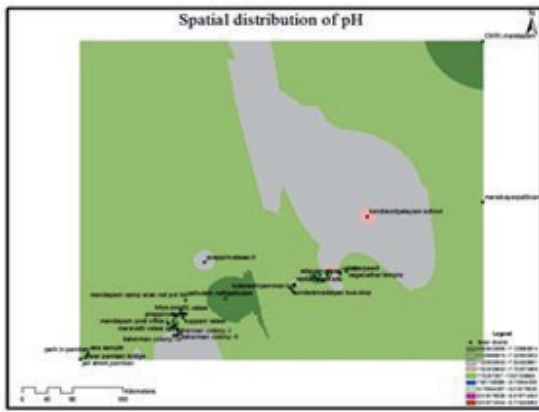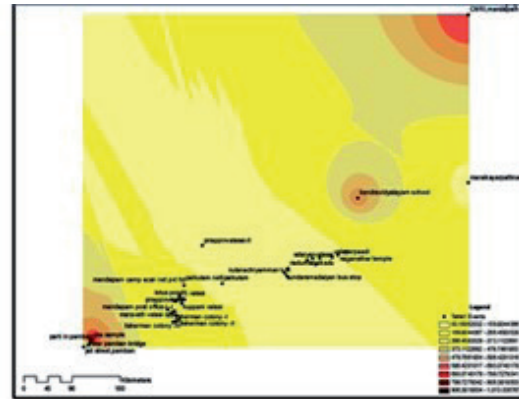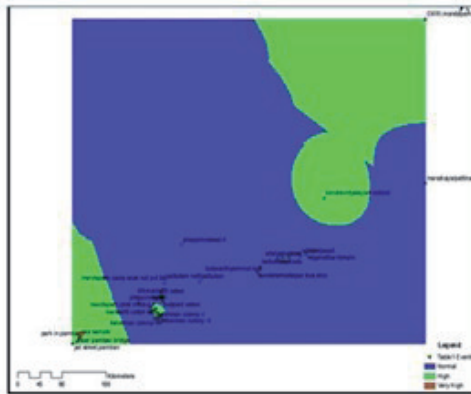
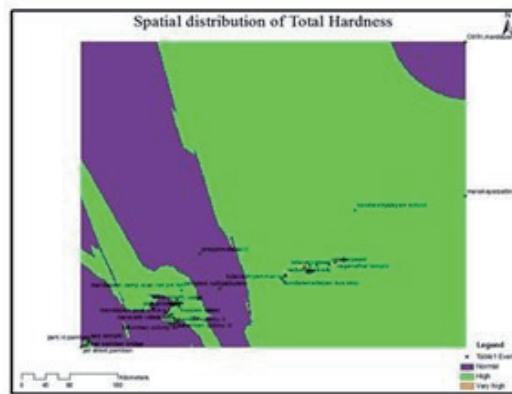(A)- Spatial Distribution of pH
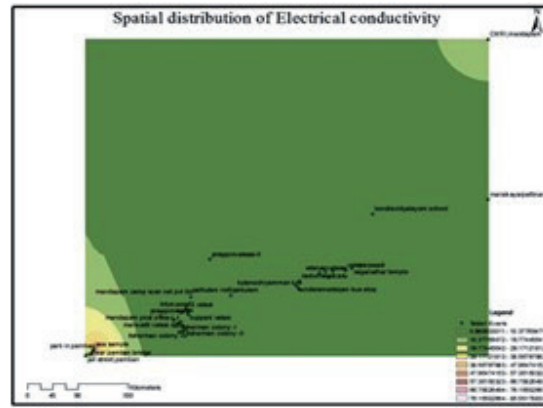


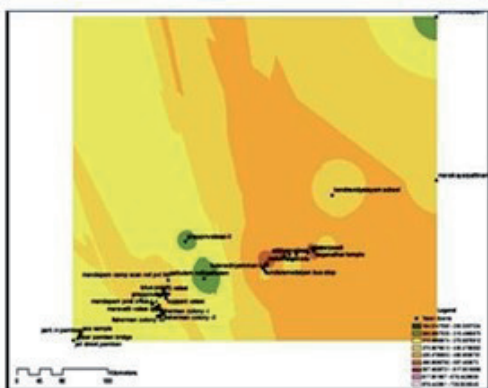(B)-Spatial Distribution of EC
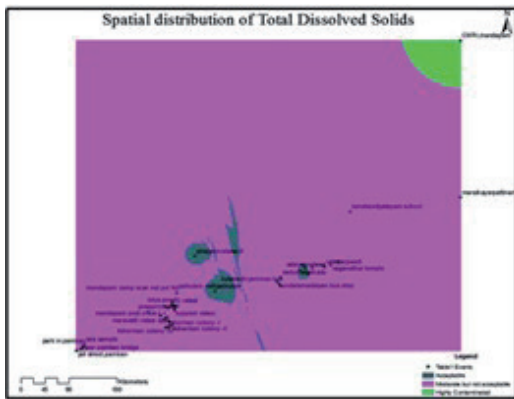


(c)- Spatial Distribution of TDS
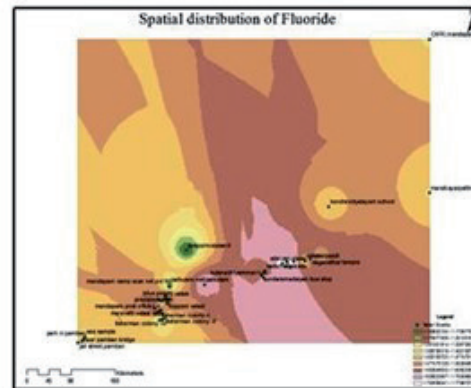


(D)-Spatial distribution of Ca2+



(E)-Spatial Distribution of Mg



(F)- Spatial Distribution of TH



(G)-Spatial Distribution of TS



(H)- Spatial Distribution of F-

Fig. 3. Spatial Distribution of water quality parameters.

## Conclusion

A wide variety of physio-chemical indicators revealed the groundwater quality in the research area is governed by the complex of seawater intrusion mechanisms. The statistical results of the Rotation component matrix demonstrated a positive loading of water quality indices. The Varimax with Kaiser Normalization statistical data in principle component analysis illustrates the standard and temporal deviations of parameters. The cluster analysis examined the relationships between spatiotemporal variability and water quality. Based on cluster condition, the range of ground water quality index found among all forty sample sites is 15% good quality, 20% medium quality, and 65% very poor-quality waters reported in coastal zone areas. According to a GIS mapping study, it also aids in water quality analysis. It indicates that the groundwater in the entire research region is not fit for direct drinking due to pH, EC, TDS, $Ca^{2+}$, $Mg^{2+}$, TH, TS, and F- levels that are not below acceptable limits in most places. The intervention and fluctuations in water quality caused by an issue with sea water infiltration, which was well predicted using GIS mapping. Understanding salinity diagram quality is made easier by the study. The floating population in the research area is increasing yearly since it is a popular destination for pilgrimages in India. Polluting activities along the coast contribute to climate change problems, which result in abrupt changes in the weather and unpredictable rainfall. To prevent pollution caused by salinization in terms of deteriorating water quality, strategies, planning, and control of groundwater use are required.

## Conflict of Interest

The authors declare no conflict of interest.

## References

1. PARDEEP KUMAR., SAUMITRA MUKHERJEE. Impact of limestone caves and seawater intrusion on coastal aquifer of middle Andaman. Journal of Contaminant Hydrology, **256**, 104197, **2022**.
2. MANSI TRIPATHI., SUNILKUMAR SINGAL Use of Principal Component Analysis for parameter selection for development of a novel Water Quality Index: A case study of river Ganga India. Ecological Indicators, **96**, 430, **2018**.
3. GUIYAO XIONG, XIAOBIN ZHU, JICHUN WU, MENGWEN LIU, YUN YAN, XIANKUI ZENG Seawater intrusion alters nitrogen cycling patterns through hydrodynamic behaviour and biochemical reactions: Based on Bayesian isotope mixing model and microbial functional network. Science of The Total Environment, **23** (3), 867, **2023**.
4. RUILIANG PU., SHAWN LANDRY A comparative analysis of high spatial resolution IKONOS and WorldView-2 imagery for mapping urban tree species. Remote Sensing of Environment, **124**, 516, **2012**.
5. CHENGPENG YUAN., YAQIANG WEI., XIAOYUN XU., XINDE CAO. Transport and transformation of arsenic in coastal aquifer at the scenario of seawater intrusion followed by managed aquifer recharge. Water Research **229**, 119440, **2023**.
6. PEIPENG WU., JEAN-CHRISTOPHE COMTE., FULIN LI., HUAWEI CHEN Influence of tides on the effectiveness of artificial freshwater injection in mitigating seawater intrusion in an unconfined coastal aquifer. Journal of Hydrology, **617**, 129043, **2023**.
7. IVAN LOVRINOVIC, VELJKO SRZIC, IVA ALJINOVIC Characterization of seawater intrusion dynamics under the influence of hydro-meteorological conditions, tidal oscillations and melioration system operative regimes to groundwater in Neretva valley coastal aquifer system. Journal of Hydrology: Regional Studies, **46**,101363, **2023**.
8. GOKHAN DEMIR GIS-based landslide susceptibility mapping for a part of the North Anatolian Fault Zone between Reşadiye and Koyulhisar (Turkey). CATENA, **183**, 104211, **2019**.
9. PADALA RAJA SHEKAR, ANEESH MATHEW Chapter 7 - Flood susceptibility mapping of the Peddavagu River Basin using GIS-AHP techniques. Developments in Environmental Science. **14,** 125, **2023**.
10. ALIREZA MOTEVALLI, HAMIDREZA MORADI, SAMAN JAVADI A. Comprehensive evaluation of groundwater vulnerability to saltwater up-coning and sea water intrusion in a coastal aquifer (case study: Ghaemshahr-juybar aquifer). Journal of Hydrology, **557**, 753, **2018**.
11. JAFAR ABU RAJAB, HESHAM EL-KALIOUBY, EID AL TARAZI, HANI AL-AMOUSH Multiscale geoelectrical characteristics of seawater intrusion along the eastern coast of the Gulf of Aqaba, Jordan. Journal of Applied Geophysics, **208**, 104868, **2023**.
12. MANSOUR SALEM ALHUMIMIDI An integrated approach for identification of seawater intrusion in coastal region: A case study of northwestern Saudi Arabia. Journal of King Saud University - Science, **32**, 3187, **2020**.
13. ANTON YUDHANA, DEDY SULISTYO, ILHAM MUFANDI GIS-based and Naive Bayes for nitrogen soil mapping in Lendah, Indonesia. Sensing and Bio-Sensing Research, **33**, 100435, **2021**.
14. BENYAPA SAWANGJANG, SATOSHI TAKIZAWA Re-evaluating fluoride intake from food and drinking water: Effect of boiling and fluoride adsorption on food. Journal of Hazardous Materials, **443**, 130162, **2023**.
15. LAMIA KOUZANA, RAMDHANE BENASSI, ABDALLAH BENMAMMOU, MENNOUBI SFAR FELFOUL Geophysical and hadrochemical study of the seawater intrusion in Mediterranean semi-arid zones. Case of the Korba coastal aquifer (Cap-Bon, Tunisia). Journal of African Earth Sciences, **58** (2), 242, **2010**.

16. CHAO YANG, QINCHUAN LI, WEI YE Dimensional synthesis method of parallel manipulators based on the principle component analysis. Mechanism and Machine Theory, **176**, 104980, **2022**.

17. MURAT COBANER, RECEP YURTAL, AHMET DOGA, LOUISH. MOTZ. Three-dimensional simulation of seawater intrusion in coastal aquifers: A case study in the Goksu Deltaic Plain. Journal of Hydrology, **65**, 262, **2012**.

18. FRANTISEK KOZISEK Regulations for calcium, magnesium or hardness in drinking water in the European Union member states. Regulatory Toxicology and Pharmacology, **112**, 130121, **2020**.

19. BARRYK LAVINE, CHARLESE DAVIDSON, JASON RITTER, DAVID J. WESTOVER, THOMAS HANCEWICZ Varimax extended rotation applied to multivariate spectroscopic image analysis. Microchemical Journal, **76** (2), 173, **2004**.

20. MANEL ELLOUZE, CHAFAI AZRI, HABIB ABIDA Spatial variability of monthly and annual rainfall data over Southern Tunisia. Atmospheric Research, **93** (4), 832, **2009**.

21. LINBO WU, LIANGTONG ZHAN, JIWU LAN, YUNMIN CHEN, SHUAI ZHANG, JUNCHAO LI, GENGQIANG LIAO Leachate migration investigation at an unlined landfill located in granite region using borehole groundwater TDS profiles. Engineering Geology, **292**, 106259, **2018**.

22. KEREN MARKS-GARBER, TALI BDOLAH-ABRAM, SAMIR NUSAIR Cluster analysis based clinical profiling of Idiopathic Pulmonary Fibrosis patients according to comorbidities evident prior to diagnosis: a single-center observational study. European Journal of Internal Medicine, **80**, 18, **2020**.

23. HENRIETTE MULLER, ULRICH HAMM Stability of market segmentation with cluster analysis – A methodological approach. Food Quality and Preference, **34**,70, **2014**.

24. IRJESH SONKER, JAYANT NATH TRIPATHI, SWARNIM Remote sensing and GIS-based landslide susceptibility mapping using frequency ratio method in Sikkim Himalaya. Quaternary Science Advances, **08**, 100067, **2022**.

25. GRECO., G. ROMANO., A. MAFFEZZOLI. Selective reinforcement of LLDPE components produced by rotational moulding with thermoplastic matrix pultruded profiles. Composites Part B: Engineering, **56**, 157, **2014**.

26. RONG WANG, BENJAMIN, YAN ZHU Heterogeneous data release for cluster analysis with differential privacy. Knowledge-Based Systems, **202**, 106047, **2020**.

27. MAJID MAHMOOD ABADI, RUHOLLAH REZAEIARSHAD Long-term evaluation of water quality parameters of the Karoun River using a regression approach and the adaptive neuro-fuzzy inference system. Marine Pollution Bulletin, **126**, 372, **2018**.

28. NURIZZAH JAMIL, FARRAHNADIA BAHARUDDIN, TENGKUSHARIFELEANI RATUL MAKNU Factors Mining in Engaging Students Learning Styles Using Exploratory Factor Analysis. Procedia Economics and Finance, **31**, 722, **2015**.

29. SIMENEH GEDEFAW ABATE, GUESH ZERU AMARE, AREGA MULU ADAL Geospatial analysis for the identification and mapping of groundwater potential zones using RS and GIS at Eastern Gojjam, Ethiopia. Groundwater for Sustainable Development, **19**, 100824, **2022**.

30. TINGTING DING, SHILIN DU, YAHUI ZHANG, HONGLIANG WANG, YUZHANG, YING CAO, JI N ZHANG, LIANSHENG HE Hardness-dependent water quality criteria for cadmium and an ecological risk assessment of the Shaying River Basin, China. Ecotoxicology and Environmental Safety, **198**, 110666, **2020**.

31. JIYANG YAN, LIFENG MA, JUAN WANG Formulation for zirconia toughened alumina (ZTA) reinforced metal matrix composites based on a three-phase concentric inclusion model, **181**, 104660, **2023**.

32. XIAOWEN ZHANG, SHUAI WEI, QIANQIAN SUN, SYEDABDUL WADOOD, BOLI GUO Source identification and spatial distribution of arsenic and heavy metals in agricultural soil around Hunan industrial estate by positive matrix factorization model, principal components analysis and geo statistical analysis. Ecotoxicology and Environmental Safety, **159**, 354, **2018**.

33. AYNUR AKTAS, DECLAN WALSH, BO HU Cancer Symptom Clusters: An Exploratory Analysis of Eight Statistical Techniques. Journal of Pain and Symptom Management, **48** (6), 1254, **2014**.

34. KAIQIANG LIU, XIAOWEI CHENG, JINGXUE LI, XIANSHU GAO, YANCA, XIAOYANG GUO, JIA ZHUANG, CHUNMEI ZHANG Effects of microstructure and pore water on electrical conductivity of cement slurry during early hydration. Composites Part B: Engineering, **177**, 107435, **2019**.

35. YIPING WU, JI CHEN Investigating the effects of point source and nonpoint source pollution on the water quality of the East River (Dongjiang) in South China. Ecological Indicators, **32**, 294, **2017**.

36. SENTHILKUMAR M., SIVASANKAR V., GOPALAKRISHNA G.V.T. Quantification of benzene in groundwater sources and risk analysis in a popular South Indian Pilgrimage City – A GIS based approach. Arabian Journal of Chemistry, **10**, S2523, **2017**.

37. JOSEPH DIEN, DANIELJ BEAL, PATRICK BERG Optimizing principal components analysis of event-related potentials: Matrix type, factor loading weighting, extraction, and rotations. Clinical Neurophysiology, **116**, 1808, **2005**.

38. WONDIM ALEMU AYENEW, HAILU AYENE KEBEDE GIS and remote sensing-based flood risk assessment and mapping: The case of Dikala Watershed in Kobo Woreda Amhara Region, Ethiopia. Environmental and Sustainability Indicators, **18**, 100243, **2023**.

39. THANDILET GULE, BROOK LEMMA, BINYAMTESFAW HAILU Implications of land use/land cover dynamics on urban water quality: Case of Addis Ababa city, Ethiopia. Heliyon, **09** (5), 15665, **2023**.

40. RUPANJALI SINGH, MAJUMDER C.B., AJITKUMAR VIDYARTHI Assessing the impacts of industrial wastewater on the inland surface water quality: An application of analytic hierarchy process (AHP) model-based water quality index and GIS techniques. Physics and Chemistry of the Earth, Parts A/B/C, **129**, 103314, **2023**.

41. YONATAN HAILU, EYOB TILAHUN, ASTIBHA BRHANE, HUSSEN RESKY, OMPRAKASH SAHU Ion exchanges process for calcium, magnesium and total hardness from ground water with natural zeolite. Groundwater for Sustainable Development, **08**, 457, **2019**.

42. SALIHA NAJIB, AHMED FADILI, KHALID MEHDI, JOELLE RISS, ABDELHADI MAKAN Contribution of hydrochemical and geoelectrical approaches to investigate salinization process and seawater intrusion in the coastal aquifers of Chaouia, Morocco. Journal of Contaminant Hydrology, **198**, 24, **2017**.

43. YATES MV On-Site Wastewater Treatment. Encyclopedia of Environmental Health, 256-63, **2011**.

44. HAHLA YASMIN, S MONTERIO, P A LIGIMOL, D D SOUZA Fluoride Contamination and Fluorosis in Gaya Region of Bihar, India. Current Biotica, **5** (2), 232, **2024**.